

Investigation of atmospheric boundary layer temperature, turbulence, and wind parameters on the basis of passive microwave remote sensing

Evgeny N. Kadygrov, Genrih N. Shur, and Anton S. Viazankin

Central Aerological Observatory, Dolgoprudny, Moscow, Russia

Received 5 March 2002; revised 10 October 2002; accepted 2 December 2002; published 12 March 2003.

[1] The MTP-5, a microwave temperature profiler, has been widely used since 1991 for investigation of the atmospheric boundary layer (ABL). The MTP-5 is an angular scanning single-channel instrument with a central frequency of about 60 GHz, designed to provide continuous, unattended observations. It can measure the thermal emission of the atmosphere with high sensitivity (0.03 K at 1 s integration time) from different zenith angles. On the basis of this measurement, it is possible to retrieve temperature profiles at the altitude range up to 600 m, to calculate wind speed and wind direction at the lowest 250 m, and to get information about some parameters of atmospheric turbulence. This report presents some applications of the MTP-5 instrument data collected in 1998–2001 within a number of international field projects: the dynamics of ABL temperature inversion in a mountain valley (Mesoscale Alpine Program (MAP)), as well as along an island coast (north part of Sakhalin Island, Russia-Japan Project); continuous measurements of the ABL temperature profile provided from a special scientific train that crossed the territory of Russia (the Transcontinental Observations of the Chemistry of the Atmosphere Project (TROICA)); and simultaneous measurements of the ABL temperature profile provided over the central and northern part of Moscow in a continuous mode (the Global Urban Research Meteorology and Environment Project (GURME)). In 1999, two MTP-5 instruments were installed on a platform that was rotating in the azimuth direction at the 310 m Obninsk Meteorological Research Tower (Meteo Tower) to validate the method and microwave equipment for measurement of wind speed and wind direction and investigation of atmospheric turbulence. Spectral analyses of the integrated signal provided an opportunity to estimate the inertial subrange low-frequency limit and its height dependence for thermal turbulence at the lowest 200 m layer. Wavelet analysis of the signal made it possible to determine the convective thermic and other coherent structures; also to estimate energy and to provide visualization of the transformation processes of those structures during changing ABL stability. For a wide spectrum of ABL models the integrated character of radiometric data is more representative than in situ data. The measurement cycle for main wind is about 45 min, with an accuracy of about 1–2 m/s for wind speed and 10–20° for wind direction. Measurements at different levels of the Meteo Tower of vertical wind speed were in good agreement with in situ data. The possibility of manufacturing the microwave instrument for simultaneous measurements of the temperature profile and wind parameters in the ABL will be also discussed in this report. *INDEX TERMS*: 6969 Radio Science: Remote sensing; 1610 Global Change: Atmosphere (0315, 0325); 3307 Meteorology and Atmospheric Dynamics: Boundary layer processes; *KEYWORDS*: microwave radiometer, MTP-5, temperature, turbulence, wind

Citation: Kadygrov, E. N., G. N. Shur, and A. S. Viazankin, Investigation of atmospheric boundary layer temperature, turbulence, and wind parameters on the basis of passive microwave remote sensing, *Radio Sci.*, 38(3), 8048, doi:10.1029/2002RS002647, 2003.

1. Introduction

[2] The investigation of atmospheric boundary layer (ABL) covers many areas (turbulence, dynamics, cloud physics, radiation, the physics of heat and mass transfer, soil physics, numerical modeling). The ABL plays an important role in many fields, including air pollution and the dispersal of pollutants, agricultural meteorology, aeronautical meteorology, mesoscale meteorology, weather forecasting, and climate studies [Garratt, 1994]. Investigation of the structure of the lower part of the ABL has mainly utilized sensors located on tower structures. For studies of the whole boundary layer, early approaches had to rely on balloon-borne instrumentation, such as free and tethered sounding balloons or constant-volume free balloons, until aircraft techniques and facilities became more widely available. However, tower and aircraft sensors are costly, and free balloons also have a high operation cost. In the last two decades or so, ABL observations have been enhanced by remote sensing techniques. These mainly involve transmitted acoustic, radio, or light energy, and the detection of the scattered energy due to natural or artificial atmospheric targets. In contrast, passive techniques involve the measurement of radiation naturally emitted from the atmosphere, for example, as in microwave and infrared radiometry. The advantages of microwave radiometric data include the possibility to provide measurements in practically all weather conditions, in urban area, its low operational cost, and continuity in time, which allows time series and time-height cross sections to be delivered [Kadygrov and Pick, 1998]. Passive microwave radiometers are very portable and can provide reliable automated continuous profiling from a variety of sites; these features are not available with the other techniques.

[3] Continuous ABL temperature profile measurements have many useful applications. Continuous measurements of ABL temperature profiles obtained by the MTP-5 in a mountain valley gave useful information for investigating the structure and evolution of ABL and its effect on alpine weather systems (Mesoscale Alpine Program (MAP), 1999, Switzerland) [Weber *et al.*, 2000]. MTP-5 data from the northern part of Sakhalin Island (Far East of Russia) were used to investigate the actual conditions of sea ice in the Okhotsk Sea and the role of sea ice in the climate system [Kadygrov *et al.*, 2000]. In 1999–2001 continuous measurements of ABL temperature profiles were provided by the MTP-5 from a special scientific train that crossed the territory of Russia from the west to the east side and from the south to the north (the Transcontinental Observations of the Chemistry of the Atmosphere Project (TROICA)). Information about the dynamics of ABL temperature inversion was very useful for investigating gas emission and aerosol distribution [Kadygrov *et al.*, 2001].

[4] Simultaneous measurements of ABL temperature profiles over the central and north parts of Moscow city and nearby area by using three MTP-5 instruments began on 1 January 2000. The measurements were provided as a part of the WMO pilot project Global Urban Research Meteorology and Environment (GURME). One of the scientific objectives of such measurements is to determine the influence of a big urban area on the ABL parameters. In addition, the Moscow Weather Forecast Bureau successfully uses MTP-5 data for its local weather forecast, for the forecast of air pollution, and for the forecast of glaze, fog and other dangerous meteorological conditions [Golitsin *et al.*, 2002].

[5] At present, microwave remote sensing of the ABL temperature has many useful applications. But practically all applications need the determination of additional parameters, such as wind parameters in the lowest part of the ABL. A standard MTP-5 instrument had to be complemented by wind speed-and-direction measurement capability. In 1997–1998, the relevant technique was developed and evaluated.

2. Features of the Scanning Radiometer

[6] A well-known microwave remote sensing method to measure temperature profiles in the troposphere used a zenith-viewing multichannel radiometer with frequencies of 53–58 GHz in the wings of the molecular oxygen absorption band [Troitsky, 1986; Westwater, 1993; Ware and Solheim, 2000]. In contrast, to measure ABL temperature profiles, we use an angular-scanning single-channel radiometer with a central frequency of 60 GHz. This method and the new instrument were proposed by Troitsky *et al.* [1993] and discussed in detail in by Kadygrov and Pick [1998] and Westwater *et al.* [1999]. Due to the large atmospheric absorption by molecular oxygen at 60 GHz, our method has some advantages for ABL temperature profiling over the multichannel method: (1) the measurements do not depend on changes of water vapor density or on the presence of fog or low clouds; (2) there is no need for calibration in the artificial microwave target (it is possible to use atmospheric emission in horizontal direction); (3) better vertical resolution in the lower 100 m; and (4) the bandwidth of the receiver is very wide (4 GHz) which provides a very high sensitivity (about 0.03 K at 1 s integration time). But the single-channel method has its limitations in altitude measurement because it measures only up to 600 m. Some difficulties are also encountered in retrieving ABL temperature profiles $T(h)$ if these have extreme spatial and temporal variations. [Kadygrov and Pick, 1998; Ivanov and Kadygrov, 1994].

[7] The microwave remote sensing method of ABL temperature profiling was realized in two types of instruments manufactured by the Russian firm ATTEX:

the ordinary version MTP-5 and the polar version MTP-5P [Westwater *et al.*, 1999]. The MTP-5P has an antenna with a 3 dB beamwidth of 0.5° and vertical resolution at the lowest altitude of about 10 m, in contrast with MTP-5 with a beamwidth of 6.0° and vertical resolution at a lowest altitude of about 50 m [Viazankin *et al.*, 2002].

3. Measurement of Wind Parameters in ABL

[8] Remote measurements of wind speed and direction obtained with a modified MTP-5 system were compared with radiosonde data and in situ measurements made by sensors mounted on platforms of the 310-m Meteorological Research Tower in Obninsk. This remote measurement system (Figure 1) can determine mean wind speed over a period of 30–60 min. in the lower 300-m atmospheric layer, with a 50-m height resolution [Viazankin *et al.*, 2001; Ivanov *et al.*, 2000].

[9] The feasibility of detecting temperature inhomogeneity in the ABL will be discussed below. A plane stratified atmospheric structure and a “frozen turbulence” hypothesis are adopted. The suggested geometry of the experiment is as follows (Figure 2).

[10] Using a radio measurement system that includes two MTP-5 instruments, simultaneous measurements are made in two directions, at the same angle α_j with the horizon and in the same mean wind vertical plane. In this way, an inhomogeneity detected by the first instrument is soon detected by the second one as well.

[11] Temperature fluctuations have quasiperiodic character and the registered signals were accepted as the set of periodic functions. In case of the presence of non-periodic background (noise or something else) the cross-correlation function of periodic and nonperiodic parts of the signal have a sharp decrease with time [Viazankin *et al.*, 1999].

[12] The cross-correlation function for signals recorded by the two instruments can be written as follows:

$$R_{xy}(\tau) = \frac{1}{2} \sum_{n=0}^N A_n B_n \cos\{\omega_n \tau + (\psi_n - \varphi_n)\}, \quad (1)$$

where A_n is the amplitude of the Fourier harmonic with frequency ω_n for a signal measured by the First instrument (subscript x), and B_n is the amplitude of the Fourier harmonic with frequency ω_n for a signal measured by the second instrument (subscript y), $\psi_n - \varphi_n$ phase difference for measured signals.

[13] The phase spectrums $\psi_n(\omega)$ and $-\varphi_n(\omega)$ are occasional but due to the “frozen turbulence” hypothesis. The phase difference includes information on propagation speed of the temperature inhomogeneities.

[14] The phase difference is given by

$$\Delta\varphi_n = \psi_n - \varphi_n = \arctg \frac{Q(\omega_n)}{C(\omega_n)}, \quad (2)$$

where the cospectrum is $C_{xy}(\omega)$ and the quadrature spectrum is $Q_{xy}(\omega)$. C_n and Q_n are the same for frequency ω_n . The corresponding harmonics amplitude is

$$A_n = \sqrt{C_n^2 + Q_n^2}. \quad (3)$$

[15] Thus, having made a standard cross-correlation analysis of a filtered signal, we obtain the set $\Delta\varphi_n, \omega_n, A_n$

$$\frac{\Delta\varphi_n}{\omega_n} = \bar{\tau}_{del}^j, \quad (4)$$

where $\bar{\tau}_{del}^j$ is the average time (to pass base l_{mid}^j at the layer Z_i , which depends on the radiation-forming layer determined by the frequency and observation angle j (Figure 2)). This time depends on the average transfer rate for the layer Z_i $u_i(z_i)$ and transfer base $l_{mid}^j(z_i)$.

[16] The transfer base $l_{mid}^j(z_i)$ at level z_i follows from simple geometry:

$$l_{mid}^j(z_i) = 2z_i \text{ctg}(\alpha_j). \quad (5)$$

Thus we obtain the set $\Delta\varphi_{n1}(\omega_{n1})$ and assign all these inhomogeneities to the first layer (subscripts $n1, i = 1, j = 1$). For the first layer and first observation angle $l_{mid}^j(z_i) = l_{mid1}^1$. If u_1 designates the transfer rate in the first layer, then

$$u_1 = \frac{l_{mid1}^1}{\bar{\tau}_{del1}^1}, \quad (6)$$

$$\text{where } \bar{\tau}_{del1}^1 = \frac{\Delta\varphi_{n1}}{\omega_{n1}}. \quad (7)$$

[17] The same analysis was done for the second scanning angle and the second layer (subscripts $n2$), and the set $(\Delta\varphi_{n2}, \omega_{n2}, A_{n2})$ was obtained. Calculation of the phase shift of inhomogeneities traveling within the first layer for the geometry of the second observation angle (Figure 3) is as follows:

$$\Delta\varphi_{n1}^2 = \frac{l_{mid1}^2 \omega_n}{u_1}, \quad (8)$$

where u_1 was found at the first experiment stage where the upper subscript denotes the number of observation angle. The first layer contribution to the integral signal will naturally decrease.

[18] In vector form, we have the following equation:

$$\vec{A}_{n2}^2 = \vec{A}_{n2} - \vec{A}_{n1}^2, \quad (9)$$



Figure 1. Remote measurement system.

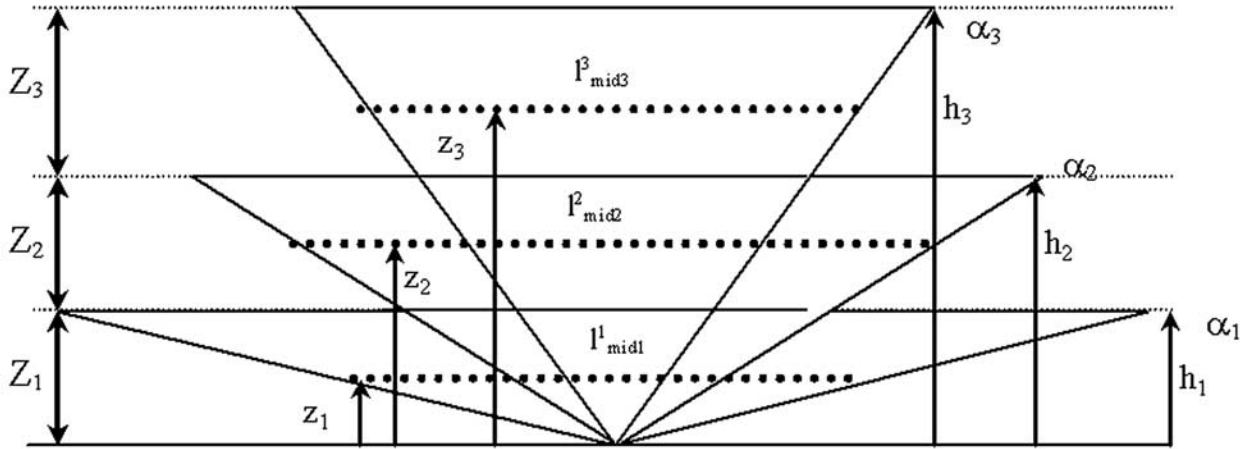


Figure 2. The geometry of the experiment (Z_i , detecting layers; α_j , observation angles; h_i , the total height of detecting layer for observation angle α_j ; z_i is the height of midpoint for layer Z_i $\{z_i = (h_{i-1} + h_i)/2, h_0 = 0\}$, l^j_{midj} average base of inhomogeneities propagation for angle j and height z_i).

where $\vec{A}_{n1}^2 = (A_{n1}^2, \Delta\varphi_{n1}^2)$ and $\vec{A}_{n2} = (A_{n2}, \Delta\varphi_{n2})$, and \vec{A}_{n2}^2 is the sought vector.

[19] The upper subscript denotes the observation angle, and the bottom subscript denotes the layer. In rectangular coordinates,

$$\vec{A}_{n2}^2 = (X_1, X_2) = (A_{n2} \cos \Delta\varphi_{n2} - A_{n1}^2 \cos \Delta\varphi_{n1}^2, A_{n2} \sin \Delta\varphi_{n2} - A_{n1}^2 \sin \Delta\varphi_{n1}^2). \quad (10)$$

$$\text{Then } A_{n2}^2 = \sqrt{X_1^2 + X_2^2}; \Delta\varphi_{n2}^2 = \text{arctg}\left(\frac{X_2}{X_1}\right). \quad (11)$$

Now, similar to the first stage, we get for the second stage,

$$u_2 = \frac{l^2_{mid2}}{\bar{\tau}_{del2}}, \quad (12)$$

where $\bar{\tau}_{del2}$ obtained from $\Delta\varphi_{n2}^2$.

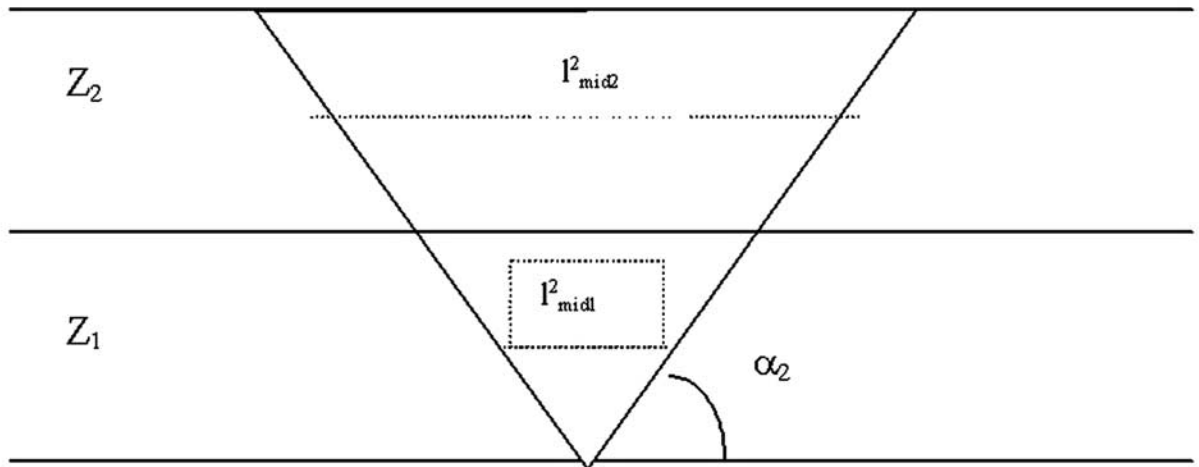


Figure 3. The experiment geometry of the second observation angle.

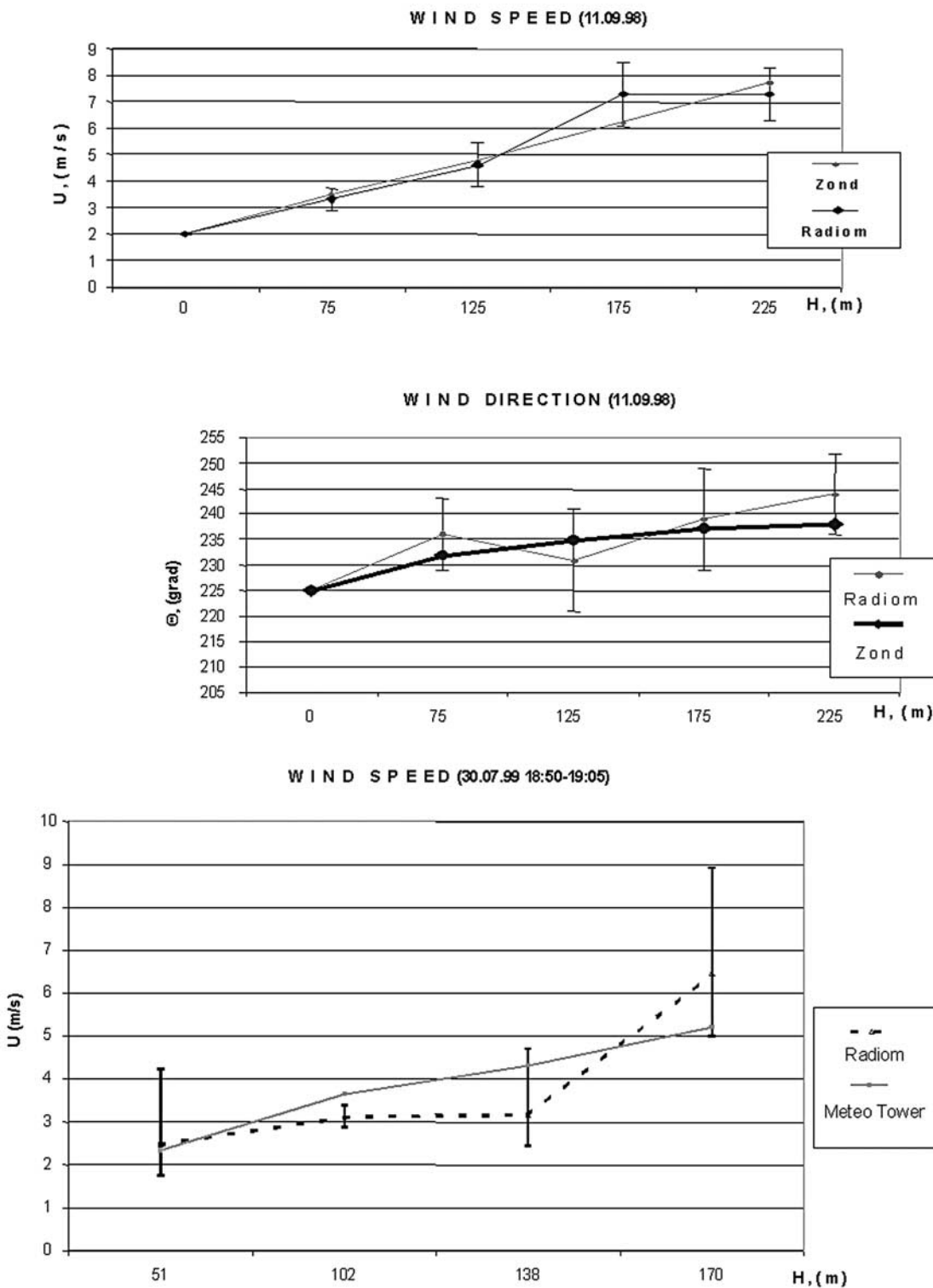


Figure 4. Comparison of microwave remote sensing data with radiosonde (wind speed, wind direction) and in situ sensors at the Meteorological Tower (wind speed).

Increment of radiobrightness temperature in unstable atmosphere and average turbulence

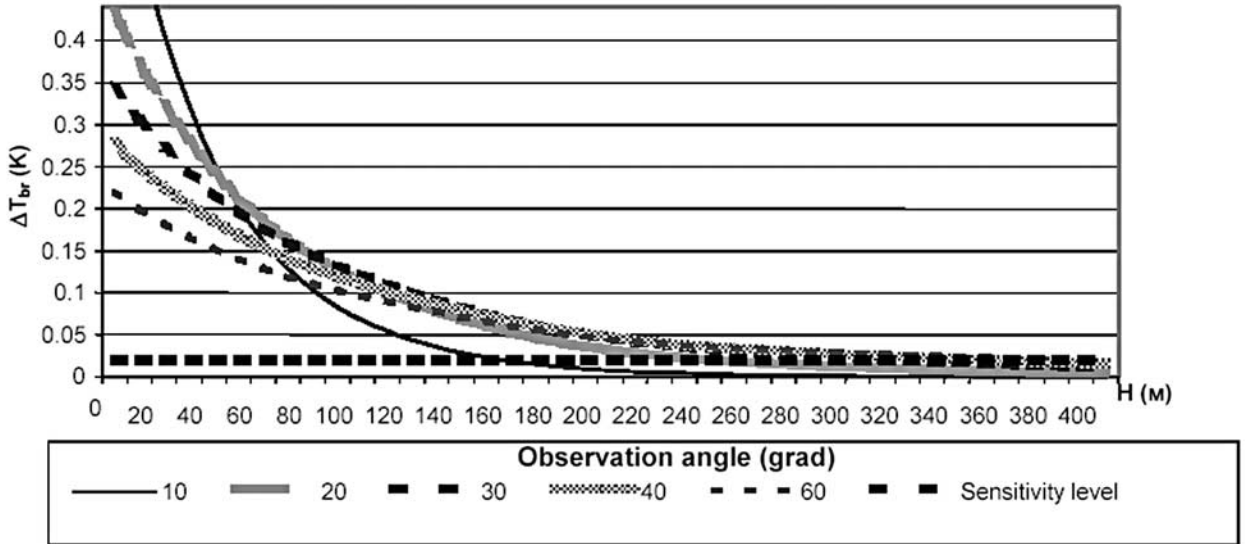


Figure 5. Increment of radiobrightness temperature in unstable conditions for average level of turbulence intensity.

[20] Figure 4 compares data obtained by the suggested spectral method with radio sounding data and with data from the Meteo Tower. Comparison of statistics from a set of 3-month continuous experimental data shows that the accuracy of microwave remote sensing measurement of wind parameters was 2 m/s in speed and 20° in direction [Viazankin *et al.*, 2001].

[21] Now we turn to the basics of a microwave passive-wind sounding technique, that is, to the possibility of detecting temperature inhomogeneities in the ABL. In terms of the theory of radio wave propagation in the atmosphere, it is useful to quote the following equation (13), which shows the presence at frequency $\nu = 60$ GHz of an unambiguous connection of radio brightness temperature fluctuations with fluctuations of the atmosphere thermodynamic temperature [Ivanov *et al.*, 2000]:

$$\delta T(\theta) = \frac{1}{\cos \theta} \int_0^{\infty} \delta T(h) W(\theta, h) Dh \quad (13)$$

where θ is the zenith observation angle ($\theta = \pi/2 - \alpha$ have been chosen for presenting of the equation (13) in the standard form); h is the height; $\delta T_{\text{r}}(\theta)$ is the detected fluctuations of radio brightness temperature; $\delta T(h)$ is the fluctuations of the atmosphere thermodynamic temperature; and $W(\theta, h)$ is the core of the integral equation.

[22] Atmospheric temperature inhomogeneities with periods of the order of 20–300-s have a spatial extension comparable with the thickness of a radiation-forming layer. This follows from Taylor’s “frozen turbulence”: $L \sim u_{\text{wind}} T$, and if $u_{\text{wind}} \sim 10$ m/s, and $T \sim 30$ s, then $L \sim 300$ m. This fact makes it possible to treat fluctuations $\delta T(h)$ as height-correlated at scales of the order of 50–100 m, which, at the receiver sensitivity ~ 0.03 K (1 s integration time), are unambiguously resolvable by the ground-based system (Figure 5).

[23] That is why the signal being recorded must carry information about turbulent temperature inhomogeneities in the lower portion of the ABL. In contrast to in situ measurements, radiometric observations are integral in nature: they are measured fluctuations of the radio brightness temperature of an atmospheric volume enclosed by the cone of an antenna radiation pattern, whose length is limited by the absorption of the medium concerned.

[24] With an antenna directed horizontally, we can detect temperature fluctuations within a horizontal volume. With an antenna directed at a large angle with the horizon, close to the zenith, we can detect temperature fluctuations of a portion of the ABL, highly averaged over the vertical. In both cases, the picture proves to be rather involved. The first problem to be solved in processing radiometric data is the discrimination of a signal that refers to the atmosphere itself.

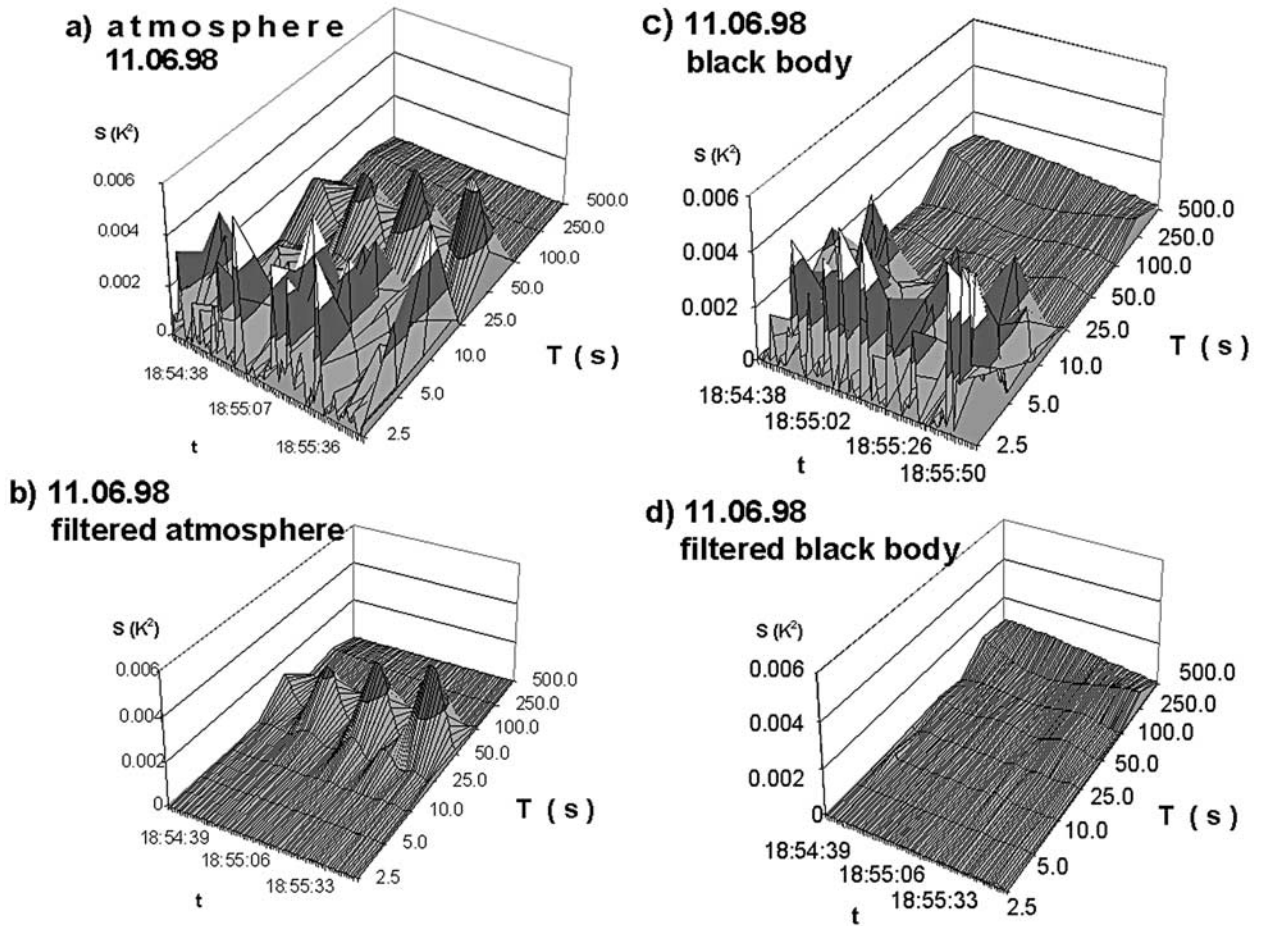


Figure 6. Energy wavelet spectrum of the detected thermal emission: (a) atmosphere, (b) filtered atmosphere, (c) black body, and (d) filtered black body.

[25] Generally, when turbulence is being investigated, measurements are made in 15–40-min. series. In studying processes with $T \sim 1$ min., the presence of noise largely complicates data reading. Therefore, to choose between frequencies, passed and filtered, correctly, it is useful to first make a wavelet analysis of the recorded signals.

[26] The wavelet method (Mexican Hat (MHAT)) [Farge, 1992] was employed:

$$(W_{\psi}f)_{a,b} = \frac{1}{\sqrt{a}} \int f(t)\psi\left(\frac{t-b}{a}\right)dt, \quad (14)$$

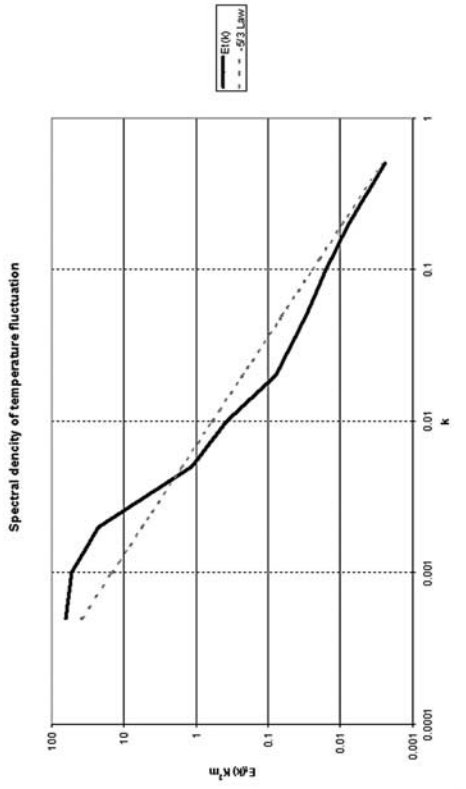
where $a,b(t) = \frac{1}{\sqrt{a}}\psi\left(\frac{t-b}{a}\right)$ is referred to as a “wavelet,” $\psi(t)$ is referred to as a “mother-wavelet,” and “a” and “b” determine the form and position of the wavelets.

[27] One can describe the space-and-time distribution of thermal energy (dispersion of temperature fluctuations)

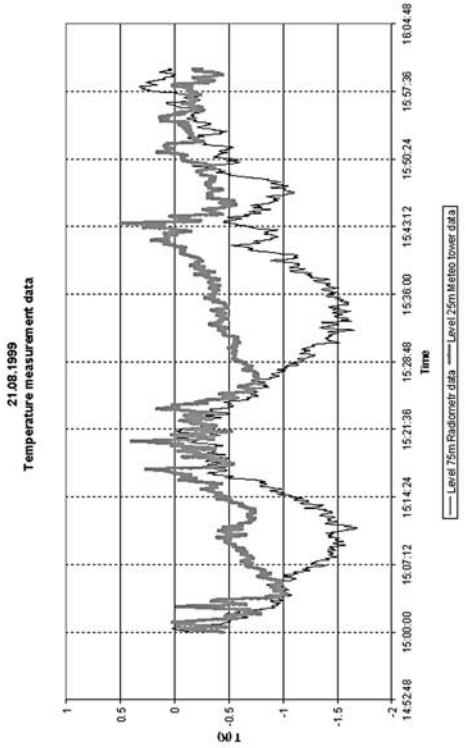
by using $W_T^2 = (W_{\psi}f)_{a,b}^2$. Hereinafter, W_T^2 will be referred to as the energy spectrum.

[28] Figure 6a shows an energy wavelet spectrum of the thermal emission detected. Figure 6b presents the same, but for the signal filtered to reduce high-frequency noise. Simultaneously, a similar instrument was covered with a standard “black body.” The wavelet spectrum of a filtered and nonfiltered “black-body” signal is shown in Figures 6c and 6d.

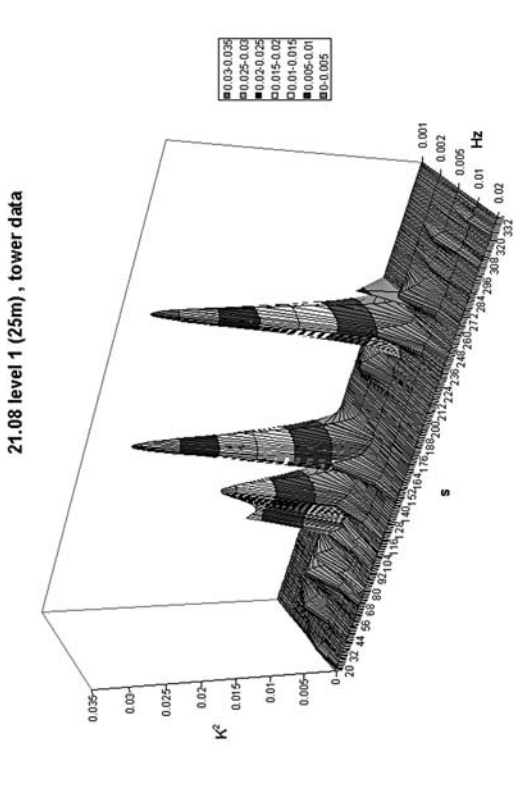
[29] Figure 6b shows readily discernible significant 25–50-s harmonics of the lag interval. Low-frequency harmonics are not resolved due to the small processing interval. In Figure 6c, these harmonics are seen to be absent. As a result, it has been demonstrated that the frequencies of thermal set noise are less than 0.1 Hz. Besides the fact that wind parameter measurements necessitate the use of detected temperature inhomogeneities, investigating the ABL



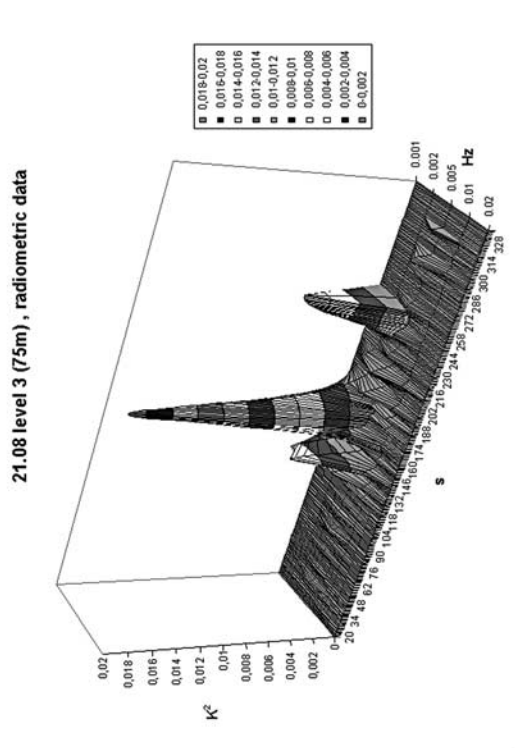
a)



b)



c)



d)

Figure 7. Temperature measured data at platform of Meteorological Tower by in situ sensors and by (a) MTP-5, (b) spectral density of temperature fluctuation and comparison with $-5/3$ law, wavelet spectrum of energy of (c) in situ and (d) microwave data.

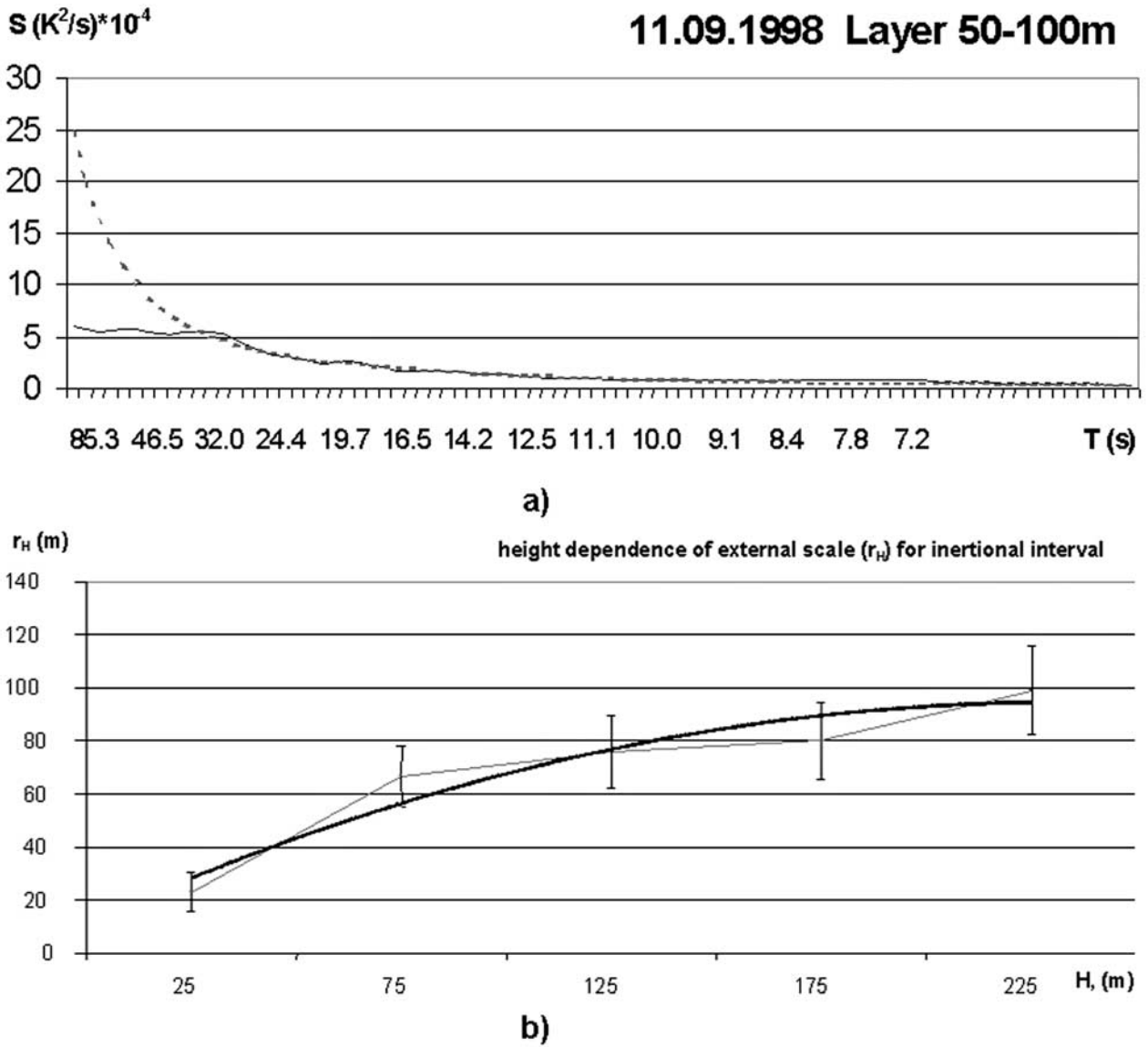


Figure 8. Comparison of calculated value of ϵ with (a) $-5/3$ law for layer 50 100 m and height dependence of external scale (r_n) for inertial interval on the base of in situ sensors data from the (b) Meteorological Tower.

temperature turbulence is of interest itself [Shur, 1993].

4. Measurement of Turbulence in ABL

[30] The horizontal sounding radiometric (MTP-5) data of 21.08.99 (15:00–16:00) were obtained in Obninsk. Figure 7a shows the behavior of temperature measured with the in situ sensor at the Meteo Tower (25 m level) and at the third platform (75-m level)

using MTP-5. Figure 7b presents a formally constructed spectral density function $E_T(k)$ (although isotropy and homogeneity conditions are not met here). It is about the same as with the $-5/3$ law.

[31] The structural constant $C_T^2 = 100 \cdot 10^{-5} \text{ deg.}^2 \text{ s.}^{-2/3}$, which, with $\bar{V} \approx 5 \text{ m/s}$, corresponds to $16 \cdot 10^{-6} \text{ deg.}^2 \text{ cm}^{-2/3}$. This is consistent with the results of conventional measurements fulfilled on the basis of in situ sensors data for the lower third of the boundary layer.

[32] Figure 7c presents the wavelet-spectrum of the square of radio brightness temperature, measured on the Meteo Tower in Obninsk, using a microwave radiometer mounted at a 75-m level with a horizontally directed antenna. It can be seen that across the antenna field of view are transferred local temperature inhomogeneities on scales of more than a hundred meters, which, as stated before, enabled the retrieval (measurement) of the wind profile by the microwave technique.

[33] From a comparison with the wavelet-spectrum of the energy measured in situ at the same time period, although at a 25-m height (Figure 7d), it is clear that the temperature structures are comparable in scale. At other Meteo Tower levels, the nature of the local structure of the thermal inhomogeneities measured by in situ sensors remains unchanged.

[34] In determining wind speed, temperature fluctuation spectra for different heights levels are obtained as intermediate results to be used in calculations. They can be employed to estimate an outer turbulence scale [Garratt, 1994]. The example of recovered spectrum for the layer 50–100 m is presented in Figure 8a. The dashed curve corresponds to the $-5/3$ law (for standard values of ϵ). These results have been calculated from observations at angles of $\alpha_1 = 10^\circ$ and $\alpha_2 = 20^\circ$.

[35] The dependence of the outer scale of the lag interval of turbulent fluctuations on height is described as follows (Figure 8b) (angles of observation are 10° , 20° , 30° , 40° , and 60° to the horizontal). To summarize, microwave measurements make it possible to obtain data on the space-and-time structure and energy of thermal turbulence in the lower portion of the ABL and, hence, to retrieve the wind speed profile.

5. Conclusions

[36] An angular-scanning microwave radiometer, with its working frequency at the molecular oxygen band center (60 GHz) can provide not only ABL temperature profile continuous measurements, but also wind parameter measurements with an accuracy of about 2 m/s in speed and 20° in direction. Measurements can be provided in all weather conditions, but the technique has limitations in altitude range (it measures up to only 600 m in temperature measurement, and up to 250 m in wind parameter measurement). The estimates of scales and temperature dispersion of turbulent thermal coherent structures, which have been performed by using of wavelet analysis shows that the 5 mm microwave technique can be also useful for investigation of atmospheric turbulence.

[37] **Acknowledgments.** This work was supported by the Russian Foundation for the Basic Investigations (Project N 01-05-64138).

References

- Farge, M., Wavelet transforms and their applications to turbulence, *Fluid Mech.*, 24, 395–457, 1992.
- Garratt, J. R., *The Atmospheric Boundary Layer*, Cambridge Atmos. and Space Sci. Ser., 316 pp., Cambridge Univ. Press, New York, 1994.
- Golitsin, G. S., E. N. Kadygrov, and I. N. Kuznetsova, Heat island above megapolicy: New results on the base of remote sensing data, *Rep. Russ. Acad. Sci.*, 385(4), 1–8, 2002.
- Ivanov, A., and E. Kadygrov, The method and technique for remote measurements of boundary layer temperature profile, *WMO Rep. N 57, Instrum. and Observ. Methods, WMO/TD N588*, pp. 407–412, World Meteorol. Org., Geneva, 1994.
- Ivanov, A., E. N. Kadygrov, and A. S. Viazankin, Combined temperature and wind microwave profiler: Results of field testing and comparison, *Rep. 74, WMO/TD-N1028*, pp. 222–225, World Meteorol. Org., Geneva, 2000.
- Kadygrov, E. N., and D. R. Pick, The potential for temperature retrieval from an angular-scanning single-channel microwave radiometer and some comparison with in situ observations, *Meteorol. Appl.*, 5, 393–404, 1998.
- Kadygrov, E. N., E. Miller, Y. Fujiyoshi, and M. Wakatsuchi, Investigation of atmospheric boundary layer thermodynamics at the Sakhalin Island by using a microwave temperature profiler, in *Proceedings of the SPIE Symposium: Microwave Remote Sensing of the Atmosphere and Environment II*, vol. 4152, pp. 310–318, Int. Soc. for Opt. Eng., Bellingham, Wash., 2000.
- Kadygrov, E. N., V. E. Kadygrov, A. D. Lykov, E. A. Miller, and A. V. Troitsky, Investigation of the atmospheric boundary layer thermodynamics on the basis of microwave remote sensing, paper presented at 11th ARM Science Team Meeting, Atlanta, Ga., U.S. Dep. Of Energy, Washington, D. C., 19–23 March 2001. (Available at http://www.arm.gov/docs/documents/technical/conf_0103/kadygrov-en.pdf.)
- Shur, G. N., Spectrum of continuous turbulence and coherent structures, *Uch. Zap. CAGI, XXIV*(3), 1993.
- Troitsky, A., Remote definition of the atmosphere temperature from spectral radiometric measurements in the line 5 mm (in Russian), *Izv. Vyssh. Uchebn. Zaved. Radiofiz.*, 29, 878–884, 1986.
- Troitsky, A., K. Gajkovich, V. Gromov, E. Kadygrov, and A. Kosov, Thermal sounding of the atmospheric boundary layer in the oxygen absorption band center at 60 GHz, *IEEE Trans. Geosci. Remote Sens.*, 31(1), 116–120, 1993.
- Viazankin, A. S., E. N. Kadygrov, A. V. Troitsky, and G. N. Shur, Investigation of temperature variations in the atmospheric boundary layer during the passage of hurricane in

- Moscow in June 1998, *Russ. Meteorol. Hydrol.*, 10, 15–24, 1999.
- Viazankin, A. S., E. N. Kadygrov, N. F. Mazurin, A. V. Troitsky, and G. N. Shur, Comparison of data on the temperature profile and its inhomogeneity structure obtained by microwave radiometer and tall meteorological tower, *Russ. Meteorol. Hydrol.*, 3, 34–44, 2001.
- Viazankin, A. S., S. A. Viazankin, E. N. Kadygrov, A. V. Koldaev, A. D. Lykov, A. F. Mironov, A. V. Troitsky, and A. N. Shaposhnikov, New microwave remote sensing ABL temperature profiler for polar region (in Russian), Paper presented at 20th All-Russia Conference of Radiowave Propagation, Russ. Acad. Sci., Moscow, 2–4 July 2002.
- Ware, R. H., and F. S. Solheim, Microwave profiling of atmospheric temperature, humidity, and cloud liquid water, in *Proceedings of the SPIE Symposium: Microwave Remote Sensing of the Atmosphere and Environment II*, vol. 4152, pp. 292–302, Int. Soc. Int. Soc. for Opt. Eng., Bellingham, Wash., 2000.
- Weber, H., M. W. Rotach, E. Kadygrov, V. Kadygrov, and E. Miller, The thermal structure of the atmospheric boundary layer in an Alpine valley: Results of continuous remote sensing measurements and comparison with radiosonde data, in *Abstracts of the International Radiation Symposium: Current Problems in Atmospheric Radiation*, pp. 234–235, St. Petersburg State Univ., St. Petersburg, Russia, 2000.
- Westwater, E. R., Ground-based microwave remote sensing of meteorological variables, in *Atmospheric Remote Sensing by Microwave Radiometry*, edited by M. A. Janssen, pp. 145–213, John Wiley, New York, 1993.
- Westwater, E. R., Y. Han, V. Leuskiy, E. N. Kadygrov, and S. A. Viazankin, Remote sensing of boundary layer temperature profiles by a scanning 5-mm microwave radiometer and RASS: Comparison experiments, *J. Atmos. Oceanic Technol.*, 16(7), 805–818, 1999.
-
- E. N. Kadygrov, G. N. Shur, and A. S. Viazankin, Central Aerological Observatory, 3 Pervomayskaya Str., Dolgoprudny, Moscow 141700, Russia. (src_attex@mtu-net.ru; VZVZVZSR@comtv.ru)